Testosterone interrupts binding of Neurexin and Neuroligin that are expressed in a highly socialized rodent, Octodon degus.

Nan Yagishita-Kyo (nanyagi@saitama-med.ac.jp)
Saitama Medical University https://orcid.org/0000-0002-9480-0003
Yuki Ikai
University of Miyazaki
Tomoko Uekita
Kyoto Tachibana University
Akio Shinohara
University of Miyazaki
Chihiro Koshimoto
University of Miyazaki
Keisuke Yoshikawa
Saitama Medical University
Kei Maruyama
Saitama Medical University
Sosuke Yagishita
Kokuritsu Seishin Shinkei Center

Research

Keywords: Octodon degus, Autism spectrum disorder, Neurexin, Neuroligin, Testosterone

Posted Date: March 16th, 2020

DOI: https://doi.org/10.21203/rs.3.rs-17382/v1

Version of Record: A version of this preprint was published at Biochemical and Biophysical Research Communications on April 1st, 2021. See the published version at https://doi.org/10.1016/j.bbrc.2021.03.015.

Abstract

Octodon degus is said to be one of the most human-like rodents because of its improved cognitive function. Notably, it has a complicated vocal communication system. Focusing on its highly developed sociality, we cloned and characterized some sociality-related genes of degus, in order to establish degus as a highly socialized animal model in molecular biology. We cloned degus Neurexin and Neuroligin as sociality-related genes, which are genetically related to autism spectrum disorder in human. They bind to each other at synaptic cleft, and this intercellular binding is also important for regulation of social behavior. Interestingly, amino acid sequences of Neurexin and Neuroligin expressed in degus brain, are highly conserved to that of human sequences. Most notably, degus Neuroligin4 is highly similar to human Neuroligin4X, which is one of the most important autism-related genes. Mouse neuroligin4 is known to be poorly similar to human Neuroligin4X, leading to the difficulty of Neuroligin4X investigation. Furthermore, our work also indicated that testosterone directly binds to degus Neurexin and intercepts intercellular Neurexin-Neuroligin binding. This effect of testosterone is unique in that it directly affects to protein function without hormone receptor signaling. Moreover, it is of high interest that testosterone is another key molecule of the higher incidence of autism in male. These results indicated that degus has the potential for animal model of sociality, and furthermore may promote understanding toward the pathogenic mechanism of autism.

Introduction

Octodon degus (degus) is a diurnal rodent endogenous to Chile (Ardiles et al., 2013; Wilson et al., 2016). Recently, degus has received considerable attention because of its high sociality (Fig. 1a). It is considered to play a critical role in social and neuro-affective research (Colonnello et al., 2011). Degus forms closely related colonies and has a complex social communication system. It has at least 15 distinct categories of audible vocalizations (Long, 2007). In order to establish degus as a highly socialized animal model in molecular biology, we cloned and characterized some sociality-related genes that are expressed in degus brain.

In this study, we report analyses of degus Neurexin (dNrxn) and Neuroligin (dNlgn). NRXN and NLGN are both single transmembrane proteins, localized at pre- and post-synapses, respectively. The Nrxn family has three genes in mammals Nrxn1, Nrxn2, and Nrxn3, all of which have longer α- and shorter β-forms. NLGN is encoded by five genes including both sex chromosomes in humans (NLGN1, NLGN2, NLGN3, NLGN4X and NLGN4Y). They all have an acetylcholinesterase-like domain. Interestingly, lack of the NLGN3, NLGN4, NRXN1 or NRXN2 proteins results in impairment of social behavior in mice (Jamain et al., 2008; Dachtler et al., 2015; Kalbassi et al., 2017). Moreover, numerous studies have identified a variety of mutations in Nlgn and Nrxn genes that range from copy number variants (Thomas et al., 1999; Jinong et al., 2006; Marshall et al., 2008; Levy et al., 2011; Sanders et al., 2011) to protein truncations and amino acid substitutions in patients with autism spectrum disorder (ASD) (Jamain et al,. 2003; Laumonnier et al., 2004; Lawson-Yuen et al., 2008; Julie et al., 2011; Yalan et al., 2012). ASD is a common neurodevelopmental disorder characterized by restricted interests, repetitive behaviors, and difficulties in

social communication. The core symptoms of ASD are impairments of language and social communication. Therefore, unraveling the molecular mechanisms of ASD onset would make a major contribution to the understanding of the neural mechanisms of sociality.

In addition, NRXN and NLGN are also known as “synaptic organizers”, and play essential roles in synapse differentiation and maturation (Graf et al., 2004; Prange et al., 2004; Kang et al., 2008), as these functions require a trans-synaptic interaction between NRXN and NLGN (Ko et al., 2009; Gokce et al., 2013; Tsetsenis et al., 2014). Furthermore, the NRXN-NLGN trans-synaptic interaction also has a crucial function in regulation of social behavior.

In this study, the gene sequences of dNlgns (dNlgn1, dNlgn2, dNlgn3, dNlgn4) and dNrxn3α were shown to be highly similar to the sequences of these genes in humans than those of mice. Most notably, the sequence of dNlgn4 is indicated to be highly similar to that of human NLGN4X; NLGN4X is one of the most important ASD-related genes (Jamain et al., 2003; Laumonnier et al., 2004; Zhang et al., 2009). We also validated the binding of dNLGN4 and dNRXN3α, and then explored novel factors that affect dNRXN3α-dNLGN4 interaction. As the dNRXN3α is structurally similar to sex hormone-binding protein, we focused on the possibility of sex hormones interacting with dNRXN3α, and their effects on the dNRXN3α-dNLGN4 interaction. Strikingly, our results showed that testosterone, one of the main male sex hormones, directly binds to dNRXN3α, and intercepts the dNRXN3α-dNLGN4 binding.

Materials And Methods

Animals

All animal experiments were carried out in accordance with the regulations and guidelines for the care and use of experimental animals at Kyoto Tachibana University and University of Miyazaki, and were approved by the institutional review committees.

Degus were housed and maintained under a 12-h light/dark cycle, at a temperature around 23 ℃ and humidity 50 % to 65 %. Two or three animals were kept in a cage with a food cup and a water bottle. Food pellets, hay cube or timothy, and water were all provided *ad libitum*.

Brain sample preparation and molecular cloning

Degus were anesthetized with sevoflurane and sacrificed. The brains were isolated and divided into hippocampus and cortices, and frozen at -80℃ until use.

Total RNA was isolated from hippocampus and cortices using TRIzol reagent (Invitrogen, CA, USA) according to the manufacturer’s instructions. cDNA was synthesized by reverse transcription of the mRNA using PrimeScript II Reverse Transcriptase (TaKaRa, Shizuoka, Japan) with Oligo$(dT)_{15}$ Primer (TaKaRa) and Random Primer (hexadeoxyribonucleotide mixture; pd $(N)_6$) (TaKaRa). The cDNA was stored at -80 ℃.

Degus neuroligins (*dNlgns*) and neurexin (*dNrxn*) genes were amplified by PCR, using the cDNA as a template. PrimeSTAR GXL DNA Polymerase (TaKaRa) or PrimeSTAR HS DNA Polymerase (TaKaRa) with PrimeSTAR GC Buffer (TaKaRa) were used for high-fidelity PCR. Primers included 5’ and 3’ ends of dNlgns or dNrxn DNA sequences, which were guided by predicted sequences of derived from *degus* genomic sequences in the NCBI database (NCBI Gene ID: 101565370, 101581175, 101568408, 101591647, 101567130).

dNlgn1 primers; 5’- atggcacttcccaggtgcat -3’ and 5’- ctataccctggttgttgaat -3’

dNlgn2 primers; 5’- atgtggctcctggcgctgtg -3’ and 5’- ctatacccgagtggtagagt -3’

dNlgn3 primers; 5’- atgtggctgcggcttggccc -3’ and 5’- ctatacccgggtggtggagt -3’

dNlgn4 primers; 5’- atgtcgaggcccaagggact -3’ and 5’- ctctagtggtggaatgtccg -3’

dNrxn3α primers; 5’- atgaccttcagtctccactc -3’ and 5’- ctacacgtagtactccttgt -3’

PCR products were inserted into pEF6/V5-His B vector (Invitrogen) at EcoRV sites using In-Fusion HD Cloning Kit (TaKaRa) or NEBuilder HiFi DNA Assembly Cloning Kit (New England Biolabs, MA, USA). The plasmids of *dNlgns* were modified by replacing V5-His tag with FLAG tag. Therefore, we obtained the following five plasmids: pEF6-dNlgn1-FLAG, pEF6-dNlgn2-FLAG, pEF6-dNlgn3-FLAG, pEF6-dNlgn4-FLAG, and pEF6-dNrxn3α-V5-His. All DNA construction experiments were carried out in accordance with the regulations and guidelines for the recombinant DNA experiments at Saitama Medical University, and were approved by the institutional review committees.

Antibodies and Chemicals

Antibodies of human proteins; Anti-NRXN3 (catalog no. HPA002727) and anti-NLGN4X (catalog no. HPA001651) were purchased from Atlas Antibodies (Bromma, Sweden). Anti-DYKDDDDK tag monoclonal antibody (mAb) was purchased from Fujifilm Wako Pure Chemical Co. (Osaka, Japan). Anti-His-tag polyclonal antibody and anti-DDDDK-tag mAb-magnetic agarose were purchased from Medical & Biological Laboratories Co., Ltd. (Nagoya, Japan). Testosterone (TSTN) solution, 5α-Dihydrotestosterone (DHT) solution, 17β-Estradiol (ESTR) solution, Progesterone (PROG) solution, and Corticosterone (CORT) solution were purchased from Cerilliant (TX, USA).

Cell culture

COS-7 cells were cultured in Dulbecco’s modified Eagle’s medium (Nacalai Tesque, Kyoto, Japan) supplemented with 10% fetal bovine serum (JRH Biosciences, KS, USA) and 1% penicillin and streptomycin (Gibco, NY, USA). Transient transfection of the cells with the plasmids was performed using Viofectin Transfection Reagent (Viogene, Taipei, Taiwan) according to the manufacturer’s instructions.

Immunoprecipitation with dNrxn3α and dNlgn4 co-transfected cells

Transfections of cells for co-immunoprecipitation was performed in a 6-well plate using 80% confluent COS-7 cells. The plasmids pEF6-dNlgn4-FLAG and pEF6-dNrxn3α-V5-His were double-transfected and after 24 h, hormones were added to the cultured medium. After 24 h of addition of hormones, the cells were harvested and lysed by 150 µl RIPA Buffer [50mM Tris-HCl buffer (pH7.6), 150mM NaCl, 1% NP-40, 0.5% Sodium Deoxycholate, 0.1% SDS] with 1% Phosphatase Inhibitor Cocktail (Nacalai Tesque) and complete EDTA-free Protease Inhibitor Cocktail (Merck, Darmstadt, Germany). After incubation at 4 ℃ for 30 min, the lysates were centrifuged at 125,000*g* for 20 min. 10 µl supernatant was taken as “input” fraction. The lysates were immunoprecipitated with anti-DDDDK-tag mAb-magnetic agarose and 500 µl Immunoprecipitation (IP) Buffer [50mM Tris-HCl (pH7.6), 150mM NaCl, 1% Triton-X 100, 1% Phosphatase Inhibitor Cocktail, cOmplete EDTA-free Protease Inhibitor Cocktail] at 4 ℃ overnight. Magnetic agarose beads were precipitated using a magnetic stand, followed by three washes with RIPA Buffer. Protein samples were denatured with 15 µl of Sample Buffer [50mM Tris-HCl (pH6.8), 2% SDS, 10% glycerol, 0.1% Bromophenol Blue, 20% 2-mercaptoethanol] and boiled for 3 min.

Co-culture for intercellular binding assay and immunoprecipitation

Transfection of cells was performed in 100 mm culture dishes using 90% confluent COS-7 cells. pEF6-dNlgn4-FLAG and pEF6-dNrxn3α-V5-His plasmids were used to transfect cells separately in various dishes. After 48 h of transfection, the cells were trypsinized, mixed, and added into 60 mm culture dishes. TSTN was added to the cultured medium. After 24 h of TSTN addition, the cells were harvested and lysed with 200 µl RIPA Buffer. The lysates were immunoprecipitated with anti-DDDDK-tag mAb-magnetic agarose and 500 µl of IP Buffer at 4 ℃ overnight. Magnetic agarose beads were precipitated using a magnetic stand, followed by three washes with RIPA Buffer. Protein samples were denatured with 15 µl of Sample Buffer and boiled for 3min.

TSTN-immobilized beads precipitation

TSTN was immobilized onto carboxylated ferrite-glycidyl methacrylate beads (Tamagawa Seiki Co., Ltd., Nagano, Japan). Transfection of cells was performed in 100 mm culture dishes using 90% confluent COS-7 cells. pEF6-dNrxn3α-V5-His plasmid was used to transfect cells. After 48 h of transfection, the cells were harvested and lysed with 600 µl RIPA Buffer. The lysates were mixed with IP Buffer and TSTN beads (10mM, 30mM), or non-immobilized beads (0mM) as negative control at 4 ℃ overnight. TSTN beads were precipitated by a magnetic stand followed by three washes with RIPA Buffer. Protein samples were denatured with 15 µl of Sample Buffer and boiled for 3 min.

Western blotting

Protein samples were separated in 5-10% precast gels (Nacalai Tesque) by SDS-PAGE and transferred onto nitrocellulose membranes. Membranes were blocked with 5% fat-free milk (MEGMILK SNOW BRAND Co., Ltd., Tokyo, Japan) for 1 h and incubated overnight at 4 ℃ with primary antibodies. Membranes were washed and probed with horseradish peroxidase-conjugated goat anti-mouse or anti-rabbit

secondary antibody. Proteins were detected using Chemi-Lumi One Super (Nacalai Tesque) or ImmunoStar LD (Fujifilm Wako Pure Chemical Co.) by ChemiDoc MP (Bio-rad Laboratories, Inc., CA, USA).

Immunocytochemistry

COS-7 cells were seeded on coverslips for an intercellular binding assay as described above and fixed in 4% paraformaldehyde containing 4% sucrose for 10 min. The cells were permeabilized with 0.3% Triton X-100 in Phosphate-buffered saline (PBS) for 10 min and blocked for 1 h in Blocking Solution (5% Normal Goat Serum, 1% Bovine Serum Albumin, 0.3% Triton X-100 in PBS). The cells were incubated with primary antibodies overnight at 4 ℃. Then, the cells were incubated with Alexa-conjugated anti-mouse or anti-rabbit secondary antibody for 2 h. Coverslips were mounted on slides using Mounting Medium [40mM Tris-HCl buffer (pH 8.5), 24% glycerol, 9.6% Mowiol 4-88, and 2.3% 1,4-diazabicyclo [2.2.2] octane (DABCO)]. Slides were visualized with an LSM 710 confocal laser scanning microscope (Carl Zeiss, Jena, Germany).

Amino acid sequence analysis and 3D structure analysis

Amino acid sequences alignment of NLGNs was performed by MEGA-X software with ClustalW using the following parameters: pairwise alignment, gap opening penalty = 10, and gap extension penalty = 0.1; and multiple alignment, gap opening penalty = 10, and gap extension penalty = 0.2. Amino acid sequences information were obtained by NCBI database (Gene ID : human 22871, 57555, 54413, 57502; marmoset 100393486, 100401738, 100385333, 100412584; naked mole-rat 101705799, 101721647, 101715602, 101715794; American beaver 109676902, 109674137, 109674385, 109679926; mouse 192167, 216856, 245537, 100113365; rat 116647, 117096, 171297; prairie vole 101999205, 101996678, 101986965, 102001548). A phylogenetic tree was inferred by using the Maximum Likelihood method and Jones et al. w/freq. model (Jones et al., 1992) with bootstraps in 500 replicates. Initial tree for the heuristic search was obtained automatically by applying Neighbor-Join and BioNJ algorithms to a matrix of pairwise distances estimated using a JTT model, and then selecting the topology with superior log likelihood value. A discrete Gamma distribution was used to model evolutionary rate differences among sites [5 categories (+G, parameter = 0.1035)]. A 3D structure model of dNrxn3α LNS domain was predicted by the SWISS-MODEL (https://swissmodel.expasy.org /interactive). A pdb file of the predicted 3D model was obtained. PyMOL was used for constructing a 3D structural drawing of dNRXN3α LNS domain and aligning 3D structures of dNRXN3α LNS1 domain and SHBG.

Statistical analysis

All statistical calculations were performed using R program (R core Team 2019). Multiple analyses were performed by Tukey's honestly significant difference test following one-way ANOVA analyses.

GenBank accession numbers of the degus genes cloned in the present report

Octodon degus neuroligin 1 (nlgn1) mRNA, complete CDS sequence, MH215558;

Octodon degus neuroligin 2 (nlgn2) mRNA, complete CDS sequence, MH215559;

Octodon degus neuroligin 3 (nlgn3) mRNA, complete CDS sequence, MH215560;

Octodon degus neuroligin 4 (nlgn4) mRNA, complete CDS sequence, MH215561;

Octodon degus nrxn3α mRNA for neurexin 3 alpha, partial cdsNrxn3α cDNA sequence, LC495319.

Results

NLGNs and NRXN3α are expressed in degus cortices and hippocampus

We synthesized cDNA from *degus* cortices and hippocampus, and amplified *dNlgns* and *dNrxns* using specific primers, which were designed using predicted sequences derived from *degus* genomic sequences. We isolated *dNlgn1*, *dNlgn2*, *dNlgn3*, and *dNlgn4*, from both cortices and hippocampus. We also identified another *dNrxn3* isoform, named as *dNrxn3α*. Amino acid sequences of *dNlgns* and *dNrxn3α* were analyzed and compared with the corresponding sequences in humans (Table 1). All dNLGN sequences are highly similar to human NLGN sequences (identity with human sequences: dNLGN1 - 98%, dNLGN2 - 98%, dNLGN3 - 99%, and dNLGN4 - 97%). Further, dNRXN3α shares 95% identity with human NRXN3α. Notably, the amino acid sequence of dNLGN4 is particularly similar to that of human NLGN4X (Fig. 1b) when compared to those of other rodents from the NCBI database, and it approaches the identity of human and marmoset (Identity with human NLGN4X: mouse - 57%, prairie vole - 36%, american beaver - 79%, naked mole-rat - 97%, marmoset - 98%). A phylogenic tree of some rodents and human concatenated NLGNs is shown (Fig. 1c). These results suggest that, in the aspect of protein sequences, *degus* is quite similar to humans than other rodents are.

Table 1. Amino acid sequences of dNLGNs and dNRXN3α are highly similar to that of human sequences.

	NLGN1	NLGN2	NLGN3	NLGN4	NRXN3α
degus	**98**	**98**	**99**	**97**	**95**
mouse	98	98	98	57	91
marmoset	99	88	97	98	88

Percentage of similarity to the human amino acid sequences of NLGNs and NRXN3α are shown.

dNLGN2 and dNLGN4 bind to dNRXN3α

We analyzed the splicing patterns of *dNlgns* and *dNrxn3α* obtained in this study (Supplemental Fig. 1). *Nlgn1* has typical splicing sites SSA and SSB, and the other *Nlgns* have the SSA site. As per our results, *dNlgn1* was SSA negative and SSB positive; similarly, *dNlgn2*: SSA+; *dNlgn3*: SSA1-, SSA2+; and *dNlgn4*: SSA-. Splicing sites of *Nrxn* are more complicated and our results indicated that *dNrxn3α* is SS1+, SS2+,

SS3+ and SS4- (Fig. 2a). We performed a binding assay of dNLGNs and dNRXN3α in a co-transfected immunoprecipitation (co-IP) assay (Fig. 2b). All dNLGNs interacted with dNRXN3α. Specifically, dNLGN2 and dNLGN4 bound strongly to dNRXN3α. Taking into account that human NLGN4X has the highest impact on ASD onset, analysis of dNLGN4 may reveal the molecular mechanism behind ASD, which remains poorly understood. Therefore, we analyzed the effect of dNRXN3α and dNLGN4 binding.

dNRXN3α shares LNS domain with human SHBG

A primary structure of dNRXN3α is shown in Fig. 2a. According to sequence alignment analysis, dNRXN3α was indicated to have six LNS domains, similar to human NRXN3α. LNS domain is named after Laminin, Neurexin, and Sex hormone-binding globulin (SHBG) from its structural similarity (Rudenko et al., 2001). The *dNrxn3α* sequence is 95% similar to human *NRXN3α* (Table 1). Therefore, the predicted 3D structure of dNRXN3α LNS domain is also similar to that of human NRXN3α. In order to determine whether the LNS domain of dNRXN3α resembles that of human SHBG, we compared 3D structures of the LNS domains (Fig. 2a). The SWISS-MODEL program was employed to generate a 3D model of dNRXN3α LNS1 domain. Then, PyMOL program was used to align the 3D models of dNRXN3α LNS1 domain and SHBG. The two protein structures are highly similar, with a root mean square deviation (RMSD) of 1.79 Å. Alignment analysis was performed and colored from RMSD by the ColorByRMSD PyMOLscript (Shandilya et al., 2012). Since SHBG interacts with sex hormones via its LNS domain (Grishkovskaya et al., 2000; Hong et al., 2015), we considered the possibility that sex hormones also bind to dNRNX3α and affect the binding between dNRXN3α and dNLGN4.

TSTN interferes with dNRXN3α-dNLGN4 binding

We analyzed whether sex hormones affect dNRXN3α-dNLGN4 binding in co-IP assay. We assayed TSTN and DHT as male hormones, and ESTR and PROG as female hormones. We also used CORT as a representative of steroid hormones. According to co-IP results, dNRXN3α-dNLGN4 binding was reduced to ~70% by TSTN addition (Fig. 2c). Hundred nanomolar TSTN sufficiently inhibited dNRXN3α-dNLGN4 binding (p = 0.044). On the other hand, ESTR, DHT, PROG and CORT had no effect on dNRXN3α-dNLGN4 binding statistically (Fig. 2d, e), even though they share a steroidal backbone with TSTN.

dNRXN3α and dNLGN4 cell-to-cell binding is interrupted by TSTN

The co-transfected IP assay cannot exclude the possibility that the binding results include intracellular dNRXN3α-dNLGN4 binding. In order to confirm that TSTN interference directly affected the intercellular dNRXN3α-dNLGN4 binding, we constructed a co-culture assay system for intercellular binding assay. COS-7 cells, expressing dNRXN3α and dNLGN4 separately, were co-cultured for observing cell-to-cell adhesion via dNRXN3α and dNLGN4. Immunocytochemistry revealed cell-to-cell attachment in our co-culture system (Fig. 3a). Interestingly, in this co-culture system, TSTN concentration-dependent decrease of dNRXN3α-dNLGN4 binding was observed (Fig. 3b). Accordingly, dNRXN3α-dNLGN4 binding was reduced to ~20% by 100 nM of TSTN (p = 0.012) (Fig. 3c). These results positively established that TSTN interferes with dNRXN3α-dNLGN4 binding intercellularly.

dNRXN3α binds directly to TSTN

To determine whether TSTN's effect on dNRXN3α-dNLGN4 binding is caused by direct binding of dNRXN3α and TSTN, we performed pull down assay of the interaction between dNRXN3α and TSTN using TSTN-immobilized beads. TSTN-immobilized beads were specially manufactured by Tamagawa Seiki Co, yielding 10mM and 30mM TSTN immobilized beads. We also used non-treated beads as negative control. dNRXN3α expressed in COS-7 cells was precipitated by TSTN-immobilized beads. Binding of dNRXN3α and TSTN was dependent on the TSTN concentration (p = 0.017) (Fig. 3d). Thus, this result showed that dNRXN3α binds to TSTN directly *in vitro*.

Discussion

dNlgn4 is highly conserved with human NLGN4X

We isolated and analyzed sequences of *dNlgns* and *dNrxn3α*. Especially, *dNlgn4* is highly similar to human *NLGN4X*. Until now, *NLGN4X* has been hardly studied, in spite of its significance to ASD onset. This is because the sequence of mouse *Nlgn4* is low similar to that of human *NLGN4X* and the expression level of mouse NLGN4 in the brain is also low (Bolliger et al., 2008; Jamain et al., 2008), leading to difficulties in mouse model investigation. The findings of this study, indicating high homology between *dNlgn4* and human *NLGN4X*, may lead to use of *degus* as an animal model. Multiple alignment and phylogenic tree analyses also show the molecular closeness between *degus* and humans. These results raise the prospect that *degus* can become a useful animal model of social and neuro-affective research, from the perspective of genetics.

TSTN interrupts dNRXN3α-dNLGN4 binding

NLGNs and NRXNs are both described as "synaptic organizers" (Graf et al., 2004; Prange et al., 2004; Kang et al., 2008). It is not until NRXNs bind to NLGNs trans-synaptically that they display their synapse-organizing abilities (Ko et al., 2009; Gokce et al., 2013; Tsetsenis et al., 2014). They bind each other at the synaptic cleft through contact between the LNS domain of NRXNs and acetylcholinesterase-like domain of NLGNs. Besides, lack of the synaptic NLGNs or NRXNs results in impairment of social behavior (Jamain et al., 2008; Dachtler et al., 2015; Kalbassi et al., 2017). On the other hand, in mice, reduction in the expression of MAM Domain Containing Glycosylphosphatidylinositol Anchor 2 (MDGA2), which interrupts NRXN-NLGN binding, impaired social interaction (Connor et al., 2016). Thus, these results indicate that a favorable balance of NRXN-NLGN binding plays an essential role in regulation of social behavior. Therefore, it is likely that dNRXN3*α*-dNLGN4 binding also plays a crucial role in synapse formation and social behavior in *degus* brain. As per our results, dNRXN3*α* also binds to dNLGN4 in cell-to-cell communication. Therefore, we explored factors which exert influence on dNRXN3*α*-dNLGN4 binding. We focused on sex hormones as candidates because of the similarity between dNRXN3*α* and SHBG.

Human SHBG binds to TSTN or other steroid hormones in comparable levels (Hong et al., 2015). Interestingly, our results indicate that TSTN binds to dNRXN3α and interrupts dNRXN3*α*-dNLGN4 intercellular adhesion, whereas DHT or ESTR do not affect dNRXN3*α*-dNLGN4 binding. TSTN, one of the main male sex hormones, has been shown to be associated with ASD onset (Ferri et al., 2018). There is a remarkable sex difference in ASD, in which the male:female ratio for children with ASD is about 4:1 or 5:1. This bias is thought to be related to fetal TSTN level (Baron-Cohen et al., 2015). A sharp rise in fetal TSTN level (so-called “androgen shower”) is important for masculinization of the male brain during the embryonic stage (Konkle and McCarthy, 2011; Roselli et al., 2011). Some studies have attributed high levels of maternally derived TSTN to higher autistic tendency (Baron-Cohen et al., 2015; Xu et al., 2015). This study suggests that the TSTN-mediated interruption of dNRXN3*α*-dNLGN4 binding may explain the molecular mechanisms of TSTN leading to aberrations in synaptic formation.

Abbreviations

Degus: Octodon degus; dNrxn: *degus* Neurexin; dNlgn: *degus* Neuroligin; ASD: Autism Spectrum Disorder; mAb: monoclonal antibody; TSTN: Testosterone; DHT: 5α-Dihydrotestosterone; ESTR: 17β-Estradiol; PROG: Progesterone; CORT: Corticosterone; PBS: Phosphate-Buffered Saline; LNS: Laminin Neurexin Sex hormone-binding globulin; SS: Splicing Site; co-IP: co-transfected Immunoprecipitation; SHBG: Sex hormone-binding globulin; RMSD: Root Mean Square Deviation

Declarations

Acknowledgements

We thank to Prof. Shoichi Ishiura (Doshisha University) for his valuable comments; Mr. Kensuke Iwasa and Dr. Shinji Yamamoto (Saitama Medical University) for laboratory maintenance; Ms. Minami Harada (Saitama Medical University) for technical supports. We also thank to staff of Division of Analytical Science (Biomedical Research Center, Saitama Medical University), and Frontier Science Research Center, University of Miyazaki for their continual supports.

Funding

This study was supported by Grant-in-Aid for Early-Career Scientists to N. Y.-K. (18K15349), SENSHIN Medical Research Foundation to N. Y.-K., Scholarship Fund for Women Researchers awarded by the Promotion and Mutual Aid Corporation for Private Schools of Japan to N. Y.-K., Internal Grant (No. 17-B-1-17), Saitama Medical University to K.M., and Grant-in-Aid for Scientific Research (C) to K. M. (18K07354).

Ethics approval and consent to participate

Not applicable.

Consent for publication

Not applicable.

Availability of data and materials

The datasets generated or analysed during the current study are available in the NCBI Nucleotide repository,

[https://www.ncbi.nlm.nih.gov/nuccore/MH215558.1;
https://www.ncbi.nlm.nih.gov/nuccore/MH215559.1;
https://www.ncbi.nlm.nih.gov/nuccore/MH215560.1;
https://www.ncbi.nlm.nih.gov/nuccore/MH215561.1;
https://www.ncbi.nlm.nih.gov/nuccore/LC495319.1]

Competing interests

The authors declare that they have no competing interests.

Authors' contributions

NY-K and SY performed the brain sample preparation and molecular cloning. TU, YI, AS, and CK reared and kept degus. NY-K performed cultured cell experiments, immunocytochemistry, and western blotting. KY and KM helped with experimental designs and data analyses. NY-K, SY, and KM wrote the manuscript, with inputs from all authors. All authors read and approved the final manuscript.

References

Ardiles AO, Ewer J, Acosta ML, Kirkwood A, Martinez AD, Ebensperger LA, Bozinovic F, Lee TM, Palacios AG. Octodon degus (Molina 1782): a model in comparative biology and biomedicine. Cold Spring Harb Protoc. 2013;2013:312-8.

Colonnello V, Iacobucci P, Fuchs T, Newberry RC, Panksepp J. Octodon degus. A useful animal model for social-affective neuroscience research: basic description of separation distress, social attachments and play. Neurosci Biobehav Rev. 2011;35:1854-63.

Long CV. Vocalisations of the degu Octodon degus, a social caviomorph rodent. Bioacoustics 2007;16:223-244

Jamain S, Radyushkin K, Hammerschmidt K, Granon S, Boretius S, Varoqueaux F, Ramanantsoa N, Gallego J, Ronnenberg A, Winter D, Frahm J, Fischer J, Bourgeron T, Ehrenreich H, Brose N. Reduced social interaction and ultrasonic communication in a mouse model of monogenic heritable autism. Proc Natl Acad Sci U S A. 2008;105:1710-5.

Dachtler J, Ivorra JL, Rowland TE, Lever C, Rodgers RJ, Clapcote SJ. Heterozygous deletion of α-neurexin I or α-neurexin II results in behaviors relevant to autism and schizophrenia. Behav Neurosci. 2015;129:765-

76.

Kalbassi S, Bachmann SO, Cross E, Roberton VH, Baudouin SJ. Male and Female Mice Lacking Neuroligin-3 Modify the Behavior of Their Wild-Type Littermates. eNeuro. 2017;4:pii: ENEURO.0145-17.2017.

Thomas NS, Sharp AJ, Browne CE, Skuse D, Hardie C, Dennis NR. Xp deletions associated with autism in three females. Hum Genet. 1999;104:43-8.

Jinong F, Richard S, Jin Y, Wenjia S, Chunmei Y, Anke B, Edwin HC, Cindy S, Charles ES, Steve SS. High frequency of neurexin 1beta signal peptide structural variants in patients with autism. Neurosci. Lett. 2006;409:10-3.

Marshall CR, Noor A, Vincent JB, Lionel AC, Feuk L, Skaug J, Shago M, Moessner R, Pinto D, Ren Y, Thiruvahindrapduram B, Fiebig A, Schreiber S, Friedman J, Ketelaars CE, Vos YJ, Ficicioglu C, Kirkpatrick S, Nicolson R, Sloman L, Summers A, Gibbons CA, Teebi A, Chitayat D, Weksberg R, Thompson A, Vardy C, Crosbie V, Luscombe S, Baatjes R, Zwaigenbaum L, Roberts W, Fernandez B, Szatmari P, Scherer SW. Structural variation of chromosomes in autism spectrum disorder. Am J Hum Genet. 2008;82:477-88.

Levy D, Ronemus M, Yamrom B, Lee YH, Leotta A, Kendall J, Marks S, Lakshmi B, Pai D, Ye K, Buja A, Krieger A, Yoon S, Troge J, Rodgers L, Iossifov I, Wigler M. Rare de novo and transmitted copy-number variation in autistic spectrum disorders. Neuron. 2011;70:886-97.

Sanders SJ, Ercan-Sencicek AG, Hus V, Luo R, Murtha MT, Moreno-De-Luca D, Chu SH, Moreau MP, Gupta AR, Thomson SA, Mason CE, Bilguvar K, Celestino-Soper PB, Choi M, Crawford EL, Davis L, Wright NR, Dhodapkar RM, DiCola M, DiLullo NM, Fernandez TV, Fielding-Singh V, Fishman DO, Frahm S, Garagaloyan R, Goh GS, Kammela S, Klei L, Lowe JK, Lund SC, McGrew AD, Meyer KA, Moffat WJ, Murdoch JD, O'Roak BJ, Ober GT, Pottenger RS, Raubeson MJ, Song Y, Wang Q, Yaspan BL, Yu TW, Yurkiewicz IR, Beaudet AL, Cantor RM, Curland M, Grice DE, Günel M, Lifton RP, Mane SM, Martin DM, Shaw CA, Sheldon M, Tischfield JA, Walsh CA, Morrow EM, Ledbetter DH, Fombonne E, Lord C, Martin CL, Brooks AI, Sutcliffe JS, Cook EH Jr, Geschwind D, Roeder K, Devlin B, State MW. Multiple recurrent de novo CNVs, including duplications of the 7q11.23 Williams syndrome region, are strongly associated with autism. Neuron. 2011;70:863-85.

Jamain S, Quach H, Betancur C, Råstam M, Colineaux C, Gillberg IC, Soderstrom H, Giros B, Leboyer M, Gillberg C, Bourgeron T. Paris Autism Research International Sibpair Study. Mutations of the X-linked genes encoding neuroligins NLGN3 and NLGN4 are associated with autism. Nat Genet. 2003;34:27-9.

Laumonnier F, Bonnet-Brilhault F, Gomot M, Blanc R, David A, Moizard MP, Raynaud M, Ronce N, Lemonnier E, Calvas P, Laudier B, Chelly J, Fryns JP, Ropers HH, Hamel BC, Andres C, Barthélémy C, Moraine C, Briault S. X-linked mental retardation and autism are associated with a mutation in the NLGN4 gene, a member of the neuroligin family. Am J Hum Genet. 2004;74:552-7.

Lawson-Yuen A, Saldivar JS, Sommer S, Picker J. Familial deletion within NLGN4 associated with autism and Tourette syndrome. Eur J Hum Genet. 2008;16:614-8.

Julie G, Tabrez JS, Peng H, Daisaku Y, Fadi FH, Nathalie C, Mathieu L, Dan S, Anne N, Ronald GL, Ferid F, Ridha J, Marie-Odile K, Lynn ED, Laurent M, Eric F, Jacques LM, Pierre D, Salvatore C, Ann MC, Guy AR. Truncating mutations in NRXN2 and NRXN1 in autism spectrum disorders and schizophrenia. Hum. Genet. 2011;130:563-73

Yalan L, Zhengmao H, Guanglei X, Yu P, Lina L, Xiaojuan X, Zhimin X, Lu X, Deyuan L, Wei L, Jingping Z, Kun X. Mutation analysis of the NRXN1 gene in a Chinese autism cohort. J Psychiatr Res. 2012;46:630-4

Graf ER, Zhang X, Jin SX, Linhoff MW, Craig AM. Neurexins induce differentiation of GABA and glutamate postsynaptic specializations via neuroligins. Cell. 2004;119:1013-26.

Prange O, Wong TP, Gerrow K, Wang YT, El-Husseini A. A balance between excitatory and inhibitory synapses is controlled by PSD-95 and neuroligin. Proc Natl Acad Sci U S A. 2004;101:13915-20.

Kang Y, Zhang X, Dobie F, Wu H, Craig AM. Induction of GABAergic postsynaptic differentiation by alpha-neurexins. J Biol Chem. 2008;283:2323-34.

Ko J, Zhang C, Arac D, Boucard AA, Brunger AT, Südhof TC. Neuroligin-1 performs neurexin-dependent and neurexin-independent functions in synapse validation. EMBO J. 2009;28:3244-55.

Gokce O, Südhof TC. Membrane-tethered monomeric neurexin LNS-domain triggers synapse formation. J Neurosci. 2013;33:14617-28.

Tsetsenis T, Boucard AA, Araç D, Brunger AT, Südhof TC. Direct visualization of trans-synaptic neurexin-neuroligin interactions during synapse formation. J Neurosci. 2014;34:15083-96.

Zhang C, Milunsky JM, Newton S, Ko J, Zhao G, Maher TA, Tager-Flusberg H, Bolliger MF, Carter AS, Boucard AA, Powell CM, Südhof TC. A neuroligin-4 missense mutation associated with autism impairs neuroligin-4 folding and endoplasmic reticulum export. J Neurosci. 2009;29:10843-54.

Jones D.T., Taylor W.R., and Thornton J.M. The rapid generation of mutation data matrices from protein sequences. Computer Applications in the Biosciences 1992;8:275-282.

R Core Team. R: A language and environment for statistical computing. R Foundation for Statistical Computing, Vienna, Austria. 2019. https://www.R-project.org/

Rudenko G, Hohenester E, Muller YA. LG/LNS domains: multiple functions -- one business end? Trends Biochem Sci. 2001;26:363-8.

Shandilya S, Vertrees J, Holder T. ColorByRMSD. 2012. https://pymolwiki.org/index.php/ColorByRMSD

Grishkovskaya I, Avvakumov GV, Sklenar G, Dales D, Hammond GL, Muller YA. Crystal structure of human sex hormone-binding globulin: steroid transport by a laminin G-like domain. EMBO J. 2000;19:504-12.

Hong H, Branham WS, Ng HW, Moland CL, Dial SL, Fang H, Perkins R, Sheehan D, Tong W. Human sex hormone-binding globulin binding affinities of 125 structurally diverse chemicals and comparison with their binding to androgen receptor, estrogen receptor, and α-fetoprotein. Toxicol Sci. 2015;143:333-48.

Bolliger MF, Pei J, Maxeiner S, Boucard AA, Grishin NV, Südhof TC. Unusually rapid evolution of Neuroligin-4 in mice. Proc Natl Acad Sci U S A. 2008;105:6421-6.

Connor SA, Ammendrup-Johnsen I, Chan AW, Kishimoto Y, Murayama C, Kurihara N, Tada A, Ge Y, Lu H, Yan R, LeDue JM, Matsumoto H, Kiyonari H, Kirino Y, Matsuzaki F, Suzuki T, Murphy TH, Wang YT, Yamamoto T, Craig AM. Altered Cortical Dynamics and Cognitive Function upon Haploinsufficiency of the Autism-Linked Excitatory Synaptic Suppressor MDGA2. Neuron. 2016;91:1052-1068.

Ferri SL, Abel T, Brodkin ES. Sex Differences in Autism Spectrum Disorder: a Review. Curr Psychiatry Rep. 2018;20:9.

Baron-Cohen S, Auyeung B, Nørgaard-Pedersen B, Hougaard DM, Abdallah MW, Melgaard L, Cohen AS, Chakrabarti B, Ruta L, Lombardo MV. Elevated fetal steroidogenic activity in autism. Mol Psychiatry. 2015;20:369-76.

Konkle AT, McCarthy MM. Developmental time course of estradiol, testosterone, and dihydrotestosterone levels in discrete regions of male and female rat brain. Endocrinology. 2011;152:223-35.

Roselli CE, Estill CT, Stadelman HL, Meaker M, Stormshak F. Separate critical periods exist for testosterone-induced differentiation of the brain and genitals in sheep. Endocrinology. 2011;152:2409-15.

Xu XJ, Zhang HF, Shou XJ, Li J, Jing WL, Zhou Y, Qian Y, Han SP, Zhang R, Han JS. Prenatal hyperandrogenic environment induced autistic-like behavior in rat offspring. Physiol Behav. 2015;138:13-20.

Figures

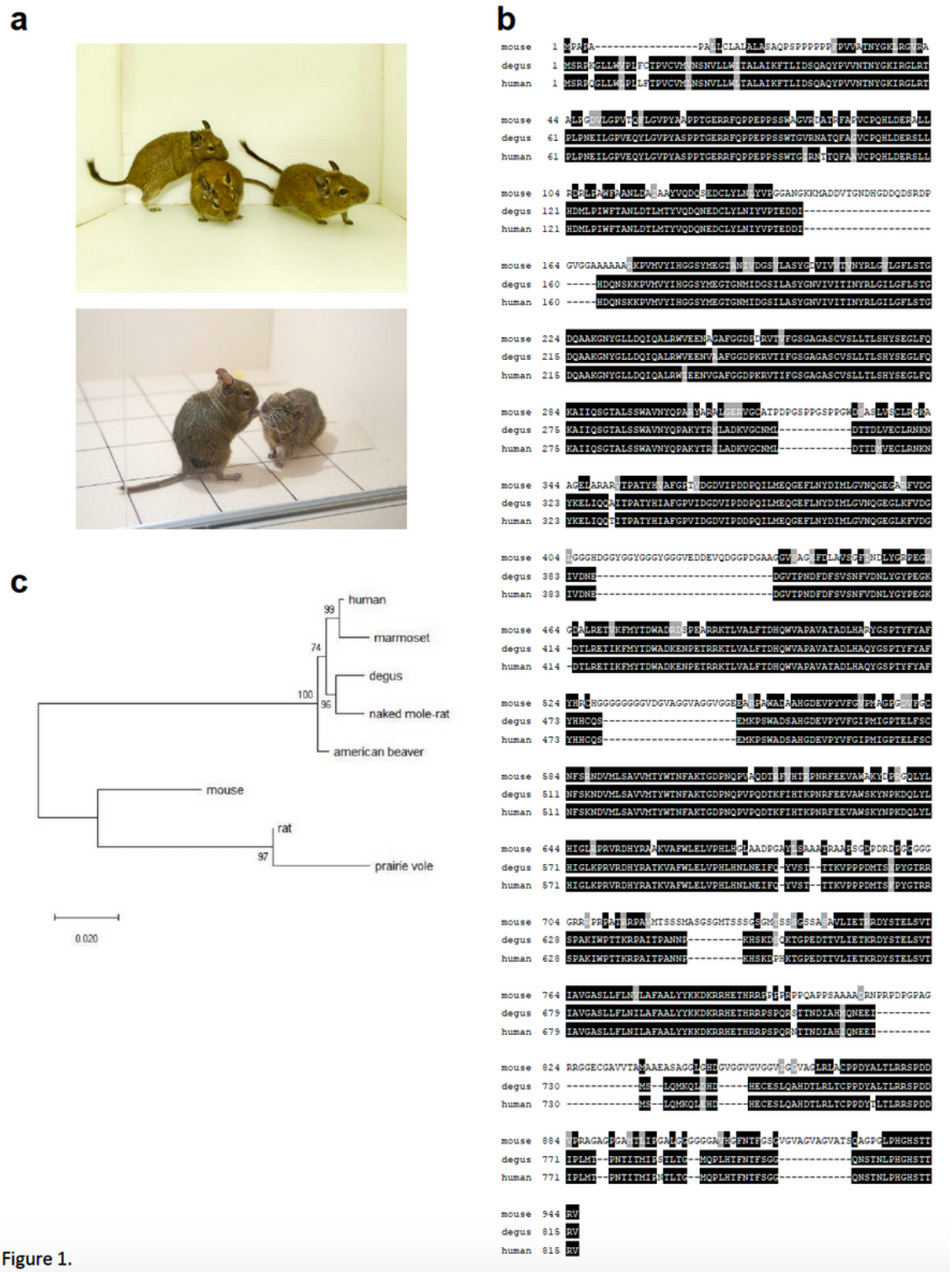

Figure 1.

Figure 1

Degus is highly socialized and dNlgn4 are similar to that of human NLGN4X. Interactions between degus individuals. (a) The amino acid sequences aligment of NLGN4. Residues shared by at least two of the three NLGN4 are boxed on a black background. (b) The phylogenic tree from concatenated NLGNs. Numbers show the bootstrap values as percentages of 500 replications. Tree was rooted with mid-point. (c)

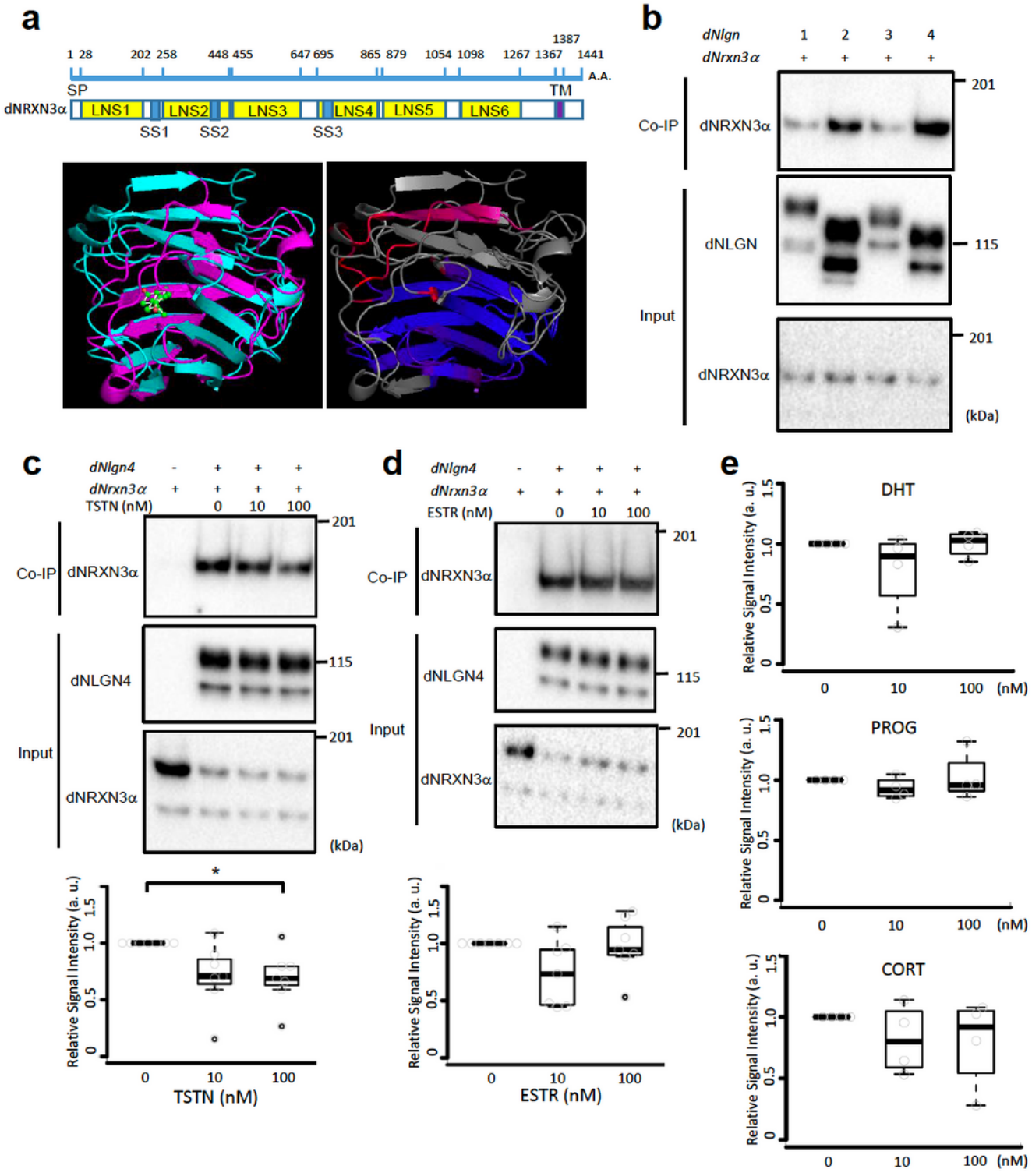

Figure 2

TSTN interferes with dNRXN3α-dNLGN4 binding. The primary structure of dNRXN3α (upper). Signal Peptide (SP), transmembrane domain (TM), Laminin Neurexin Sex hormone-binding globulin (LNS) domain, and spliced site (SS) are indicated. The predicted 3D structure of dNRXN3α LNS1 domain (magenta) and 3D structure of SHBG (cyan) (lower, left). Alignment of colored from RMSD (Superimpose was performed using “colorbyrmsd” script in Pymol; blue = lowest RMSD; pink = highest RMSD, gray =

not used in superimpose.) (lower, right). (a) Represntative blots of co-IP assay with dNLGN1, dNLGN2, dNLGN3, dNLGN4 and dNRXN3α. (b) co-IP assay of dNLGN4 and dNRXN3α with TSTN addition (upper). A box plot is shown in lower (n = 7). (c) co-IP assay of dNLGN4 and dNRXN3α with ESTR addition (upper). A box plot is shown in lower (n = 7). (d) Box plots of co-IP with DHT, PROG and CORT (n = 4). (e) *p < 0.05

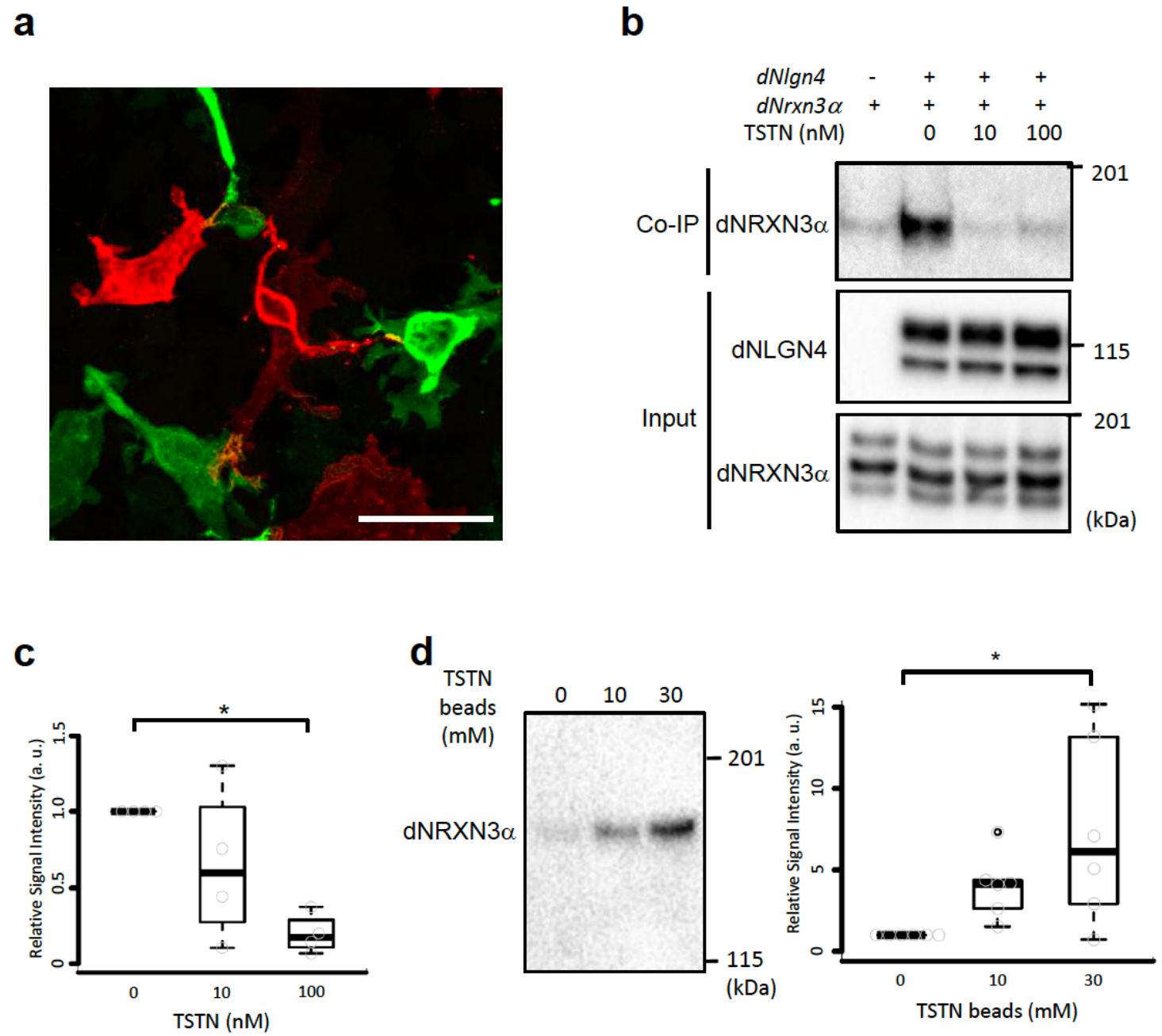

Figure 3

dNRXN3α and dNLGN4 cell-to-cell binding is interrupted by TSTN. Representative figure of intercellular binding of dNRXN3α (Green) and dNLGN4 (Red). Bar : 50mm (a) co-IP assay of intercellular binding of dNRXN3α and dNLGN4 with TSTN addition. (b) A box plot of intercellular binding of dNRXN3α and dNLGN4 with TSTN addition (n = 4). (c) Pull down assay of dNRXN3α with TSTN-immobilized beads. A representative blot is shown in left. A box plot is shown in right (n = 6). (d) *p < 0.05

Supplementary Files

This is a list of supplementary files associated with this preprint. Click to download.

- SupplementalFigure1.pdf